Germination-induced modifications of starch structure, flour-processing characteristics, and *in vitro* digestive properties in maize

Lipeng Liu [a,b], Xin Jiang [a,b], Yelinxin Chen [a,b], Sanabil Yaqoob [a,b], Lin Xiu [a,b], Huimin Liu [a,b], Mingzhu Zheng [a,b], Dan Cai [a,b,*], Jingsheng Liu [a,b,*]

[a] *College of Food Science and Engineering, Jilin Agricultural University, Changchun, Jilin 130118, China*
[b] *National Engineering Research Center for Wheat and Corn Deep Processing, Changchun, Jilin 130118, China*

ARTICLE INFO

ABSTRACT

Current research on maize germination suffers from long sampling intervals, and the relationship between the starch structure and the processing properties of flour in maize is still unclear. This study observed the effect of germination on the structure and composition of maize starch and the processing properties of maize flour over a 72 h period using a short interval sampling method. At 36 h, the short-range ordered structure, crystallinity, and enthalpy of starch reached the highest values of 1.02, 34.30%, and 9.90 J/g, respectively. At 72 h, the ratios of rapidly-digested starch (RDS) and slowly-digested starch (SDS) enhanced to 29.37% and 28.97%; the RS content reduced to 35.37%; and the flow properties of the starch were improved. This study enhances the understanding of the effects of germination on the processing properties of maize starch and flour, determines the appropriate application, and recommends the use of germination in the food industry.

1. Introduction

In addition to being one of the top three cereal crops in Asia, maize is an important source of food and crucial for economic growth in Africa, Latin America, and the Caribbean (Prasanna et al., 2020). In the previous decade, global maize production increased due to a combination of rising demand, technological advancements, enhanced yields, and expanded acreage, thereby becoming the most widely grown and traded crop in the subsequent decade. Sugars, fats, proteins, and fibers play crucial roles in a healthy diet. Maize is a good source of these nutrients. Starch is one of the primary sources of energy. Maize starch is also often used as a stabilizer, gelling agent, emulsifier, and thickener in the food, papermaking, pharmaceutical, and feed processing industries. Moreover, starch is also often used as a nanocarrier to encapsulate specific bioactive compounds in the field of medicine. For instance, highly branched maize starch was used as a nanocarrier for embedding and releasing ascorbic acid, which strengthened its photo and thermal stabilities (Gu, Chen, & Tian, 2021). In addition, there is a direct relationship between the structural properties of maize starch and the processing characteristics and nutritional composition of maize. Therefore, understanding the structure of maize starch is essential for the food industry and for improving human health.

Germination is the process in which, following dormancy, grains with a specific germination potential absorb water and undergo a series of metabolic activities and morphological changes under favorable conditions. The emergence of radicles and plumules during germination results from the reactivation of seed metabolism. Some researchers have used non-targeted and targeted flavoring agents to understand the impact of different germination days on changes in the flavor composition of roasted barley malt; elucidated the critical effects of lipid oxidation and non-enzymatic browning reactions on the formation of barley malt flavor; and found that an appropriate germination time leads to a richer flavor composition of roasted barley malt (Gu, Jin, Schwarz, Rao, & Chen, 2023). Moreover, the type and content of flavor-related compounds in germinated chickpeas, lentils, and soybeans changed due to altered levels of lipoxygenase and free radicals at different stages of germination, and the undesirable odors in germinated legumes-based products can be reduced by controlling the germination conditions (Xu, Jin, Gu, Rao, & Chen, 2020). Germination can markedly enhance the activity of amylase in millet, resulting in the breakdown of large starch molecules into smaller ones along with structural modifications (Sharma & Gujral, 2020). In addition, post-germination, the water-absorption capacities of these plants improved (Xu et al., 2019). In wheat, brown rice, and triticale, germination confers enhanced functional

---

characteristics to the whole flour, including increased oil absorption, enhanced foaming ability, and improved emulsifying properties, among other noteworthy effects. Under an extended period of germination, substantial changes occur in the crystallinity, short-range ordered structure, and particle size of quinoa starch, which influence the structure of the starch aggregates (Xing et al., 2021). In germinating zinc-enriched brown rice, the hydrolysis rate of starch increased with germination time, and at 34 h, the rate was 2.77% higher than that of the ungerminated rice (Wang, Chen, He, Zhan, & Bai, 2022). Similarly, the peak and final viscosities of glutamate isolate starch after 48 h of germination were reduced by ~18.83% and 16.05%, respectively, and the enthalpy by ~19.28% compared with that of ungerminated starch (Liu et al., 2022). Thus, the activity of endogenous enzymes within the seeds elevates during germination. This phenomenon results in the decomposition of complex biomolecules such as starch, lipids, and proteins into smaller molecules such as glucose, amino acids, and peptides, which serve as essential nutrients and energy sources for subsequent growth and development, altering the biochemical composition of the seed.

Currently, the primary methods of starch modification involve physical and chemical approaches. Using sequential ethanol fractionation to extract the debranched, waxy maize starch, it was found that the thermostability of the starch was improved, and the content of slow-digesting starch (SDS) and resistant starch (RS) was enhanced (Zhang et al., 2024). In contrast, germination, a natural process that alters starch structure, is largely unexplored. Unlike conventional starch modification by physical and chemical methods, germination is more energy- and cost-efficient and can effectively improve the nutritional value and functional properties of grains. Additionally, germination can alter the composition and ratio of amino acids, diminish the levels of anti-nutritional factors, and elevate the bioavailability of nutrients in grains.

"Germination" usually refers to the process of emerge from the seed stage, whereas "sprouting" usually refers to the stage of cotyledon growth from the time the buds are released to the ground, focusing more on germ growth (Gan et al., 2017). This study examined the relationship between the structure of maize starch and its thermal, pasting, and digestive properties, as well as the elemental composition and processing properties (including pasting and thermal properties) of whole maize meal at different germination times, using short interval sampling. The results show an obvious correlation between the starch structure and the processing properties of the flour in maize during germination, thus providing a theoretical basis for the use of germination as a processing method in food production.

2. Materials and methods

2.1. Materials

Yellow maize 'Jidan 66' (harvested at maturity in October 2021) (moisture 10.40 ± 0.29 g/100 g, amylose 25.68 ± 0.56 g/100 g, amylopectin 47.78 ± 0.32 g/100 g) was provided by the National Engineering Research Centre for Wheat and Corn Deep Processing, Jilin Agricultural University, Jilin, China. KBr, α-amylase (sourced from the porcine pancreas [10 U/mg]), and amyloglucosidase (sourced from *Aspergillus niger* [260 U/mL]) were purchased from Sigma-Aldrich, St. Louis, MO, USA. NaOH, H_2SO_4, NaAc, TCA, and other reagents were of analytically pure grade.

2.2. Maize germination

Maize kernels were germinated according to the method described by Su et al. (2020) with slight modifications. About 100 g of maize kernels were soaked in 1% NaOCl for 30 min. Subsequently, the maize kernels were transferred to a $34 \times 25 \times 4.5$ cm germination tray and soaked in distilled water for 6 h. The germination was carried out in an incubator under dark at 25 °C and 75% relative humidity. The water in the trays was changed every 12 h to ensure optimal conditions. At the end of the germination phase, samples were collected every 6 h from 0 to 72 h. The collected samples were then rinsed with distilled water and then dried at 40 °C.

2.3. Maize meal preparation and starch isolation

First, the germinated maize grains were mixed with distilled water in a ratio of 1:4, and then a high-speed blender was used to obtain a maize slurry. The resultant pulp was then filtered through 50- and 200-mesh filters and kept aside for 6 h for sedimentation. The supernatant was slowly poured out, centrifuged at 5000*g* for 15 min, and the precipitated, top, soft, yellow starch layer was scraped out. This procedure was repeated a minimum of three times or until the precipitated starch exhibited almost no color change. The starch was then dried at 45 °C and stored in a dryer. After germination, the maize grains were dried in an oven at 45 °C, crushed using a universal crusher, sieved through an 80-mesh screen, and stored.

2.4. Determination of the elemental composition of maize

The total starch content of the germinated-maize flour was measured utilizing commercially available kits (Megazyme International Ireland Ltd., Wicklow, Ireland). Protein, ash, moisture, and fat contents in the germination-maize flour were determined using the method by Association of Official Analytical Chemists (AOAC, 2006). The Kjeldahl method was used to ascertain the total energy content of protein, the scorching method for the ash content, the direct drying method for the moisture content, and the Soxhlet extraction method for the fat content. Furthermore, the reducing sugar content was ascertained using a commercially available kit (Shanghai Yuanye Bio-Technology Co. Ltd., Shanghai, China).

2.5. Amylase and protease assays

The amylase activity was assayed using a commercially available kit (Shanghai Yuanye Bio-Technology Co. Ltd.). In addition, the protease activity was measured per the method reported by Wang et al., 2020, Wang et al. (2020), Wang et al., 2020 with minor modifications. Briefly, ~ 2.5 g of germinated maize kernels were homogenized using phosphate buffer at 4 °C under refrigerated conditions. The volume was then adjusted using a volumetric flask to 25 mL. Subsequently, Tyr was used to plot a standard curve for measuring the variations in enzyme activity during maize germination. Casein was used as the substrate to quantify the changes in proteolytic activity throughout the process. The undigested proteins were precipitated with 10% TCA by incubating the reaction mixture at room temperature for 10 min. The color was developed using the Folin's reagent, and the OD_{680} was measured. The Tyr concentration was then determined based on the OD values. A Unit (U) was defined as the amount of Tyr produced from the hydrolysis of casein in 1 min, yielding 1 μg of tyrosine.

2.6. Surface morphology

The surface of the dried maize starch was sputter-coated with gold and photographed using a Sigma 300 scanning electron microscope (Carl Zeiss AG, Oberkochen, Germany) at magnifications of 1500 and 5000×.

2.7. X-ray diffraction (XRD)

The XRD experiments were carried out in a manner similar to the approach outlined by Chen et al. (2018), with a few minor adjustments. In this study, starch samples were examined using an XRD-6100 X-ray diffractometer (Shimadzu, Kyoto, Japan), operated at 40 kV and 40 mA

Cu-Kα radiation. The measurements were conducted at room temperature and a scan rate of 2°/min from 5° to 40°. The diffractograms acquired were processed using Jade 6.5 (Materials Data Inc., Livermore, CA, USA) to determine the relative crystallinity. The formula used was:

$$X_c = \frac{A_c}{A_c + A_a} \times 100\% \tag{1}$$

X_c denotes the relative crystallinity of the sample; A_a and A_c denote the area of the amorphous and crystalline regions in the diffractogram, respectively.

2.8. Fourier transform infrared (FT-IR) spectrometry

The FT-IR spectrometry was conducted in accordance with the method described by Ma, Chen, Wang, Chen, and Zhang (2023), with minor modifications. Under IR light, ~ 2 mg of the sample was weighed and thoroughly mixed with dry KBr powder using a mortar and pestle in a ratio of 1:100. The resultant mixture was pelletized using a pellet press, and the obtained pellet was used to acquire spectral data in the λ range of 4000–400 cm^{-1}. The short-range ordered structure of starch was calculated using 1047 cm^{-1}/1022 cm^{-1}.

2.9. Thermal properties

The differential scanning calorimetry (DSC) studies were conducted per the method described by Najib, Heydari, Tu, and Meda (2023) with minor modifications. The thermal properties of maize starch were determined using a Q2000 DSC (TA Instruments, New Castle, DE, USA). Maize starch and flour samples were mixed with distilled water in an Al crucible at a ratio of 1:3 and equilibrated at room temperature for 12 h. The measurement was carried out at a programmed heating rate of 10 °C/min and a scanning range of 30–120 °C. The crucible without the samples was used as a reference.

2.10. Rapid visco analyzer (RVA)

The RVA parameters were determined with the help of the RVA-TecMaster (Perten Instruments AB, Sweden). For this, ~ 3 ± 0.02 g of the starch or maize-flour sample was weighed and added to an Al RVA box, to which 25 mL of pure water was then added to prepare a mixed system. A paddle was used to stir the starch suspension at 960 rpm for 10 s before switching to 160 rpm until the program's completion. The suspension was warmed to an equilibrium temperature of 50 °C and maintained for 1 min, then heated to 140 °C at a rate of 6 °C/min and maintained for 5 min. Next, it was cooled down to 50 °C at a rate of 6 °C/min and incubated for 4 min.

2.11. Rheological properties of maize starch

The rheological properties were measured using an MCR302 rheometer (Anton Paar Co., Graz, Austria) following a previously described procedure (Hao et al., 2024). The maize starch paste was placed on the rheological platform. The plate was a CP-50 conical plate with a diameter of 50 mm and a plate spacing of 0.05 mm; the plate was set to 25 °C, the strain was set to 1%, and the range of measurement was 0.1–10 Hz. At these parameters, the loss modulus (G'), storage modulus (G"), and loss angular tangent (tan δ) with the angular frequency changes of the starch were determined. Similarly, the shear rate was tested by a gradual shear from 0 to 300 s^{-1} and then from 300 to 0 s^{-1}. The data obtained were fitted with the Power-Law equation (y = ax^k).

2.12. In vitro starch digestibility

The method described by Englyst, Kingman, and Cummings (1992) was used to determine the *in vitro* digestibility of maize starch. A 50 mL beaker containing ~3.0 g of α-amylase was placed on a scale and added with 10 mL of 0.1 mol/L sodium acetate buffer (pH 5.4). The mixture was thoroughly mixed using a magnetic stirrer and then centrifuged at 5000 *g* for 10 min. Subsequently, 1.0 mL of glucoamylase was added to the supernatant to obtain a solution containing both enzymes. The procedure was completed by adding a screw-cap tube with ~0.5 g of the starch sample and then filled with 8.5 mL of 0.1 mol/L sodium acetate buffer (pH 5.4). Subsequently, 2.5 mL of the combined enzyme solution was added, along with five glass beads. The tube was then submerged in water at 37 °C and oscillated at 200 g for a predetermined period. The enzymes were deactivated at 20 and 120 min by removing 500 μL of the supernatant and adding 25 mL of 90% ethanol. The glucose concentration of the supernatant was then determined using a glucose detection kit (Yuanye).

$$RDS\ (\%) = \frac{(G_{20} - G_0) \times 0.9}{TS} \times 100\% \tag{2}$$

$$SDS\ (\%) = \frac{(G_{120} - G_{20}) \times 0.9}{TS} \times 100\% \tag{3}$$

$$RS\ (\%) = 1\text{-RDS-SDS} \tag{4}$$

TS denotes the total starch content in the sample (mg); RDS denotes the rapidly-digested starch content (mg); SDS denotes the slowly-digested starch content (mg); and RS denotes the resistant starch content (mg).

2.13. Hydration and gelling properties

The water absorption index (WAI), water solubility index (WSI), and swelling potential (SP) of the whole maize flour post-germination were determined following the methodology established previously (Bravo-Núñez & Gómez, 2019). For each measurement, 1 g of maize or germination maize flour was separately weighed and placed into a 50 mL centrifuge tube. A 5% emulsion was prepared by adding 20 mL of distilled water and thorough mixing by continuous shaking. Subsequently, the tube was placed in a water bath at 30 °C for 30 min and ensured shaking every 5 min. Next, the tube was cooled to room temperature and centrifuged at 5000 *g* for 15 min. The supernatant was carefully transferred to a small Al container and dried at 110 °C until a constant weight was achieved. The separate masses of the dried material and precipitate were then weighed.

$$WAI\ (g/g) = \frac{m_2}{m} \tag{5}$$

$$WSI\ (g/g) = \frac{m_3}{m} \tag{6}$$

$$SP\ (g/g) = \frac{m_2}{m - m_3} \tag{7}$$

m denotes the sample quality (g); m_2 denotes the sediment quality (g); and m_3 denotes the mass of solids in supernatant (g).

2.14. Statistical analysis

The results of the study are reported as the mean ± standard deviation. Statistical analysis of variance (ANOVA) was conducted using the SPSS 22.0 software (IBM, Armonk, NY, USA) to analyze the data. Additionally, Tukey's Honest Significant Difference (HSD) was used for statistical ANOVA, with a significance level set at 0.05. Origin 2018 (https://www.originlab.com/2018) was used to plot the data.

3. Results and discussion

3.1. Elemental composition and enzyme activities

Table 1 depicts the dynamic changes in the fundamental chemical

Table 1
Changes in essential components and key enzyme activities during maize germination.

sample	Moisture (g/100 g)	Protein (g/100 g)	Fat (g/100 g)	Ash (g/100 g)	Starch (g/100 g)	Reducing sugar (g/100 g)	Amylase activity (U/ g)	Protease activity (U/ g)
0 h	20.87 ± 1.38[i]	8.74 ± 0.10[e]	5.25 ± 0.13[a]	1.75 ± 0.04[a]	73.46 ± 0.64[a]	1.68 ± 0.03[a]	2.01 ± 0.07e	5.58 ± 0.17e
6 h	23.56 ± 0.33[h]	8.89 ± 0.05[de]	5.12 ± 0.27[a]	1.69 ± 0.06[a]	69.46 ± 1.78[ab]	1.69 ± 0.06[a]	2.62 ± 0.07e	5.76 ± 0.39de
12 h	26.25 ± 0.12[g]	8.95 ± 0.04[cde]	4.72 ± 0.04[ab]	1.68 ± 0.20[a]	67.95 ± 1.38[abc]	1.71 ± 0.09[a]	2.39 ± 0.05e	5.87 ± 0.14de
18 h	27.71 ± 0.16f[g]	9.00 ± 0.01[c]	4.84 ± 0.12[ab]	2.00 ± 0.50[a]	65.19 ± 2.53[bcd]	1.66 ± 0.03[a]	2.47 ± 0.18e	6.38 ± 0.49cde
24 h	28.68 ± 0.25[ef]	9.24 ± 0.09[c]	4.86 ± 0.05[ab]	1.81 ± 0.23[a]	66.13 ± 1.36[bcd]	2.14 ± 0.04[b]	5.98 ± 0.16 cd	7.06 ± 0.20bc
30 h	30.00 ± 0.86[de]	9.87 ± 0.04[b]	4.64 ± 0.43[ab]	1.61 ± 0.05[a]	61.76 ± 2.99[de]	1.98 ± 0.01[b]	5.80 ± 0.58d	7.79 ± 0.96bc
36 h	31.04 ± 0.79[cd]	10.15 ± 0.07[a]	4.67 ± 0.43[ab]	1.82 ± 0.09[a]	62.67 ± 2.57[cde]	2.51 ± 0.07[c]	8.52 ± 1.02b	8.08 ± 0.10b
42 h	32.45 ± 0.62[c]	9.70 ± 0.14[b]	4.64 ± 0.43[ab]	1.19 ± 0.06[a]	59.16 ± 0.94[e]	3.54 ± 0.12[d]	7.34 ± 0.41bc	7.73 ± 0.58bc
48 h	35.36 ± 0.48[b]	9.07 ± 0.09[cd]	4.60 ± 0.23[ab]	1.14 ± 0.24[a]	57.68 ± 0.64[e]	4.03 ± 0.17[e]	7.86 ± 0.48bc	7.02 ± 0.59bc
60 h	36.84 ± 0.40[b]	8.96 ± 0.02[cde]	4.46 ± 0.11[ab]	1.26 ± 0.03[a]	48.22 ± 0.71[f]	4.54 ± 0.08[f]	8.28 ± 0.62b	8.08 ± 0.08b
72 h	40.45 ± 0.69[a]	8.92 ± 0.14[cde]	3.88 ± 0.60[b]	1.23 ± 0.11[a]	44.97 ± 0.72[f]	4.92 ± 0.05[g]	15.28 ± 0.08a	10.56 ± 0.25a

constituents and activities of key enzymes during germination in maize between 0 and 72 h. Starch and lipids are the two primary sources of energy for metabolic activities in plants. Consequently, the breakdown products of these compounds enter the tricarboxylic acid (TCA) cycle to provide vital energy for growth and development. As a result, the total amount of starch and lipids was inversely proportional to the germination time, unlike the concentration of reducing sugars. This trend indicates that during germination, starch was partially hydrolyzed and converted into saccharides, which provided the materials for growth. In addition, during respiration and other metabolic processes, a portion of the mineral elements are utilized and assimilated into cellular structures, resulting in a reduction in the overall ash content. Furthermore, as germination progressed, the crude protein content initially increased, followed by a decline. This trend may be attributable to the ribosomes attaching to the endoplasmic reticulum to initiate protein synthesis and the proteins accumulating within specific organelles during the early stages of germination. Nonetheless, during the later stages, insoluble starch and proteins are hydrolyzed into soluble forms such as sugars and amino acids for efficient transport to the embryo, thus satisfying the growth needs of maize kernels. This metabolism is the principal reason for the observed elevation in the activities of proteins and starch-degrading enzymes during the germination of maize kernels.

3.2. Microscopic morphological observations

Fig. 1 depicts the microstructural changes in maize starch following germination. The overall form of the starch granules comprised a sphere with an irregular block structure and a relatively smooth surface. Following germination, the surface of some granules became rougher, and the number of pits and the surface area increased. The small surface pits are likely the result of hydrolysis by amylase, which was activated during re- germination (Zhang et al., 2022). However, the shape of a majority of the starch molecules was retained or was only slightly altered.

The hydrolysis of starch is catalyzed by α- and β-amylases, debranching enzyme, and α-glucosidase (Oliveira, Coimbra, Galdeano, Carvalho, & Takeiti, 2020), which occurs in three stages. First, the enzyme diffuses onto the starch surface, forming depressions; then, the enzyme molecules bind to sites on the starch and adsorb to initiate hydrolysis; and finally, the hydrolysis accelerates, creating pores and facilitating the perfusion of the enzyme to the inside of the granules (Zhang et al., 2022). Consequently, at 36 h of germination, the surface became markedly more porous (Fig. 1D). This phenomenon allowed an increase in the enzyme–starch contact area, making it easier for the

amylase to bind to the surface, facilitating the entry of the enzyme molecules through the pores formed, thereby accelerating the rate of hydrolysis, and creating more numerous and dense pores.

3.3. Crystalline structure

The characteristic XRD peaks of maize starch, which represent a unique molecular characteristic of the A-type starch, were observed at 15°, 17°, 18°, and 23° (Fig. 2A). Furthermore, there was no discernible change in the positions of the starch-related peaks post-germination, indicating that germination did not affect its crystal structure. This observation was consistent with the previous research findings (Nieves-Hernández et al., 2023). The crystallinity of the maize kernel starch reached the highest of 33.23% at 48 h of germination, which was an increase of 9.35% compared to untreated samples. However, the crystallinity reduced after 48 h and reached 23.51% at 72 h. A similar outcome was observed in the starch of germinating mung beans (Liu et al., 2020). This pattern may be due to the enzyme attacking the amorphous zone of the starch during the initial stages of germination, resulting in a relative increase in the area of the crystallization zone. However, as germination progressed, the enzyme entered the interior of the starch granules through the surface pores, hydrolyzing the crystalline zone, resulting in a tendency for the crystallinity to increase initially and then decrease. It has been hypothesized that the variations in the relative abundance and length of branched-chain amylopectin influence the differences in the crystallinity of starch (Ma, Liu, Liu, Zhang, & Liu, 2020). This change occurring during early germination may also be related to H-bonding and hydrophobic interactions within the starch molecules. Higher crystallinity can harden the starch gel more, contributing slightly to the improvement of the mechanical properties of the starch. The possible use of starch from germinating maize as an additive to improve the rheological and mechanical properties of foods can be widened in some respects (Ran & Yang, 2022).

3.4. Short-range ordered structure

Fig. 2B illustrates the FT-IR spectra of starch at different stages of germination, while Fig. 2C presents the FT-IR spectra with Fourier deconvolution from 1200 to 800 cm⁻¹. A crucial factor in determining the short-range orderliness of starch is the comparison of the absorbance intensity at the two specific wavenumbers, 1047 and 1022 cm⁻¹, of the IR spectrum (Bai et al., 2023). The former indicates the extent of ordered structure, whereas the latter is commonly linked to the amorphous region of starch (Wang, Shi, et al., 2020; Wang, Xiao, et al., 2020; Wang,
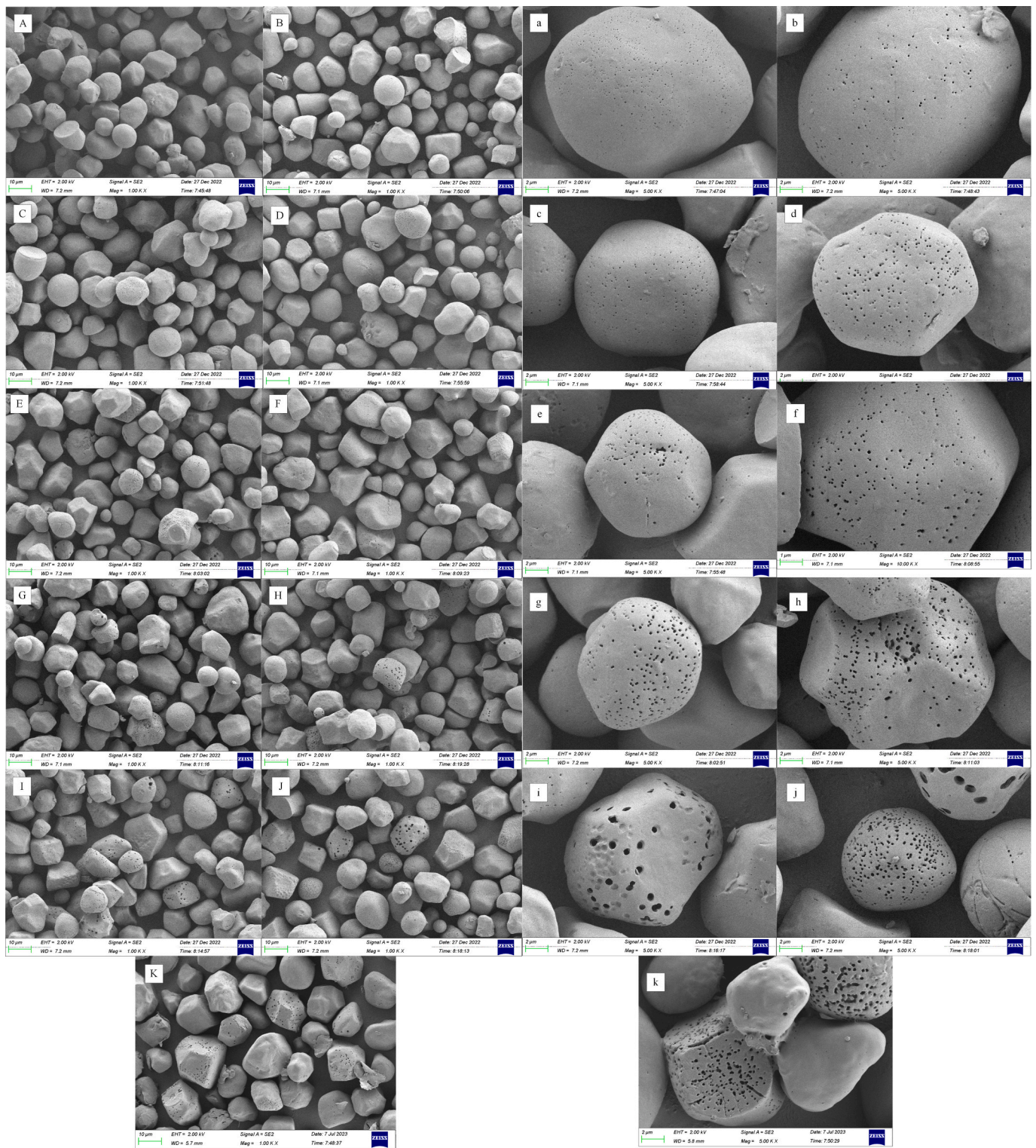
Fig. 1. SEM images of the maize starch during germination 0–72 h: magnification values 1000× (A-K), 5000× (a-k).

The short-range ordered structure initially increased and then decreased as the germination progressed (Table 2), with the peak value achieved at 36 h, indicating the maximum level of stability. Consequently, the 1047/1022 ratio diminished, which can be attributed to the hydrolysis of starch during germination, most likely catalyzed by endogenous enzymes. Initially, these enzymes disrupt the disordered structure of the starch surface, reorganizing the linear surface molecules.

In summary, this research demonstrates that the short-range orderliness of maize starch is influenced by germination time. The highest structural stability was observed at 36 h, with a subsequent decrease in the 1047/1022 ratio, indicating a decline in structural order. This phenomenon is likely due to enzymatic hydrolysis. Initial disruption of the disordered structure leads to a rearrangement of the surface molecules, which results in an enhancement in the short-range ordered structures during the early stages of germination. However, as the
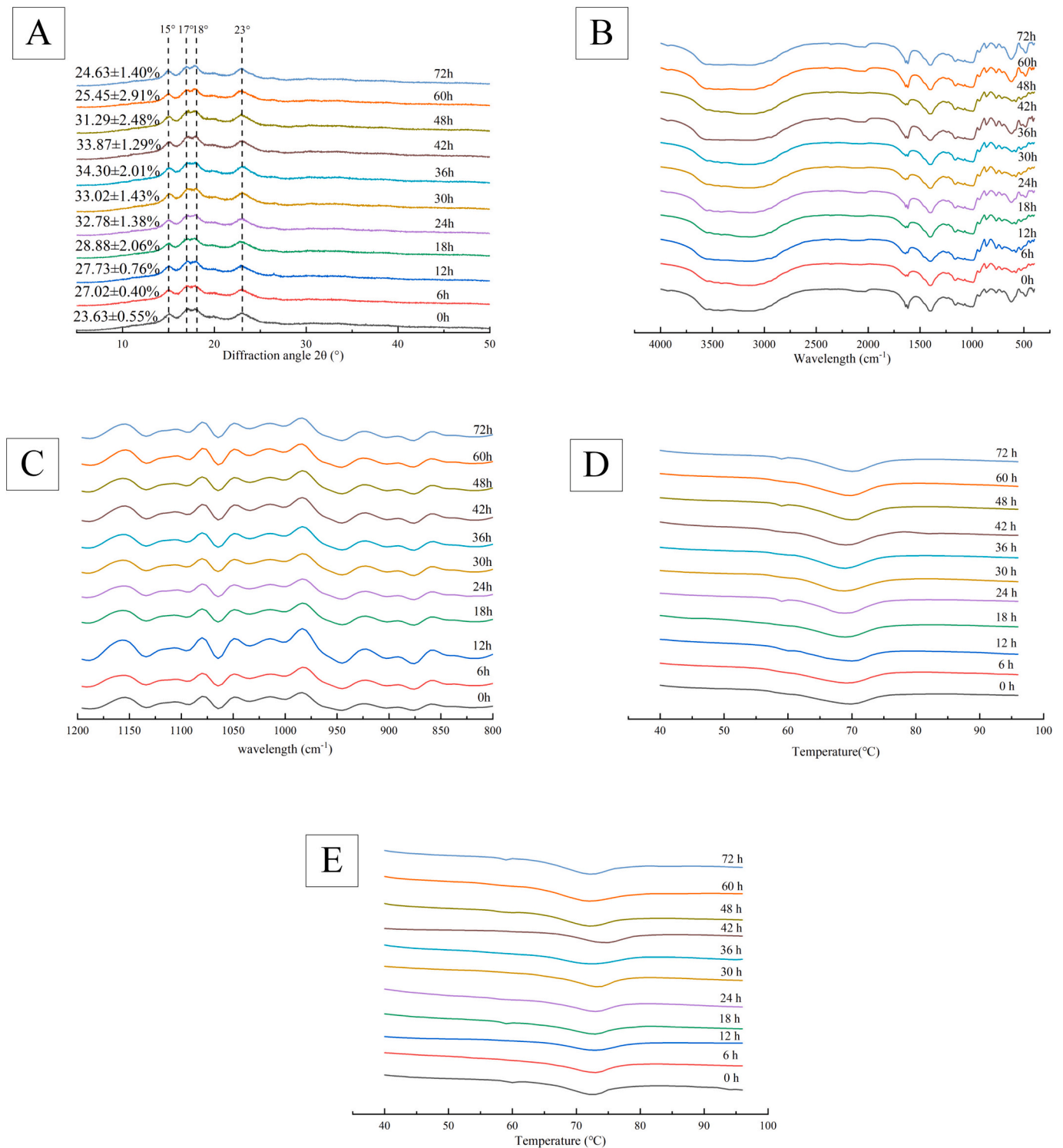
Fig. 2. XRD patterns of the maize starch (A); FT-IR spectra of the maize starch in the range of 4000 cm^{-1}–400 cm^{-1} (B) and 1200 cm^{-1}–800 cm^{-1} (C); DSC curves (D) of the maize starch during 0–72 h of germination. DSC curves (e) of the maize flour during 0–72 h of germination.

duration of germination increased, the hydrolysis of the starch intensified, leading to a decline in the short-range order after 36 h. This result is consistent with the previous XRD-based findings of enhanced crystallinity, which are believed to represent the long-range ordered structure of starch. Thus, during the initial stages of maize germination, the ordered structure of starch molecules increases to a certain extent, indicating an enhancement in the stability of the molecular structure. However, excessively long germination can also collapse the ordered

structure.

3.5. Thermal properties

Fig. 2C, Fig. 2D, and Table 2 depict the thermodynamic characteristics of maize starch and flour at different germination durations. The change in enthalpy (ΔH) indicates the amount of energy required to disrupt the double helix structure in the crystalline region of starch

Table 2
Short-range orderliness and thermal property parameters of maize starch with different germination times.

Sample	Germination time	$R_{1047/1022}$	Relative Crystallinity(%)	ΔH (J/g)	T_p (°C)	T_o (°C)	T_c (°C)
Starch	0 h	0.97 ± 0.00^e	23.63 ± 0.55^d	-6.01 ± 0.10^e	69.20 ± 0.00^{de}	56.87 ± 0.14^d	75.37 ± 0.19^d
	6 h	0.97 ± 0.01^e	27.02 ± 0.40^{cd}	-6.62 ± 0.07^{de}	69.44 ± 0.00^c	60.38 ± 0.20^a	76.56 ± 0.12^{bc}
	12 h	0.97 ± 0.00^e	27.73 ± 0.76^{bcd}	-6.29 ± 0.45^e	69.25 ± 0.01^d	57.86 ± 0.27^{cd}	76.53 ± 0.14^{bc}
	18 h	0.99 ± 0.00^c	28.88 ± 2.06^{abcd}	-7.37 ± 0.27^c	68.99 ± 0.00^f	59.25 ± 0.29^{ab}	76.78 ± 0.43^b
	24 h	1.00 ± 0.00^{bc}	32.78 ± 1.38^{ab}	-7.55 ± 0.42^c	69.17 ± 0.02^e	58.91 ± 0.36^{bc}	76.53 ± 0.29^{bc}
	30 h	1.01 ± 0.00^{ab}	33.02 ± 1.43^{ab}	-7.91 ± 0.07^{bc}	68.83 ± 0.03^g	59.39 ± 0.15^{ab}	77.86 ± 0.14^a
	36 h	1.02 ± 0.01^a	34.30 ± 2.01^a	-9.90 ± 0.16^a	68.83 ± 0.00^g	59.14 ± 0.26^{ab}	77.91 ± 0.21^a
	42 h	0.99 ± 0.00^{cd}	33.87 ± 1.29^a	-8.39 ± 0.05^{bc}	69.28 ± 0.00^d	59.55 ± 0.20^{ab}	$78.05 \pm 0.14a$
	48 h	0.98 ± 0.00^{de}	31.29 ± 2.48^{abc}	-7.78 ± 0.05^{bc}	69.91 ± 0.02^a	59.44 ± 0.27^{ab}	77.19 ± 0.24^b
	60 h	0.97 ± 0.00^{de}	25.45 ± 2.91^d	-7.91 ± 0.12^b	69.48 ± 0.01^c	56.82 ± 0.21^d	77.99 ± 0.14^a
	72 h	0.95 ± 0.00^f	24.63 ± 1.40^d	-7.15 ± 0.29^{cd}	69.96 ± 0.05^a	58.97 ± 0.48^{bc}	77.00 ± 0.15^b
Maize flour	0 h			-1.95 ± 0.15^f	71.95 ± 0.41^{de}	65.56 ± 0.25^a	77.34 ± 0.55^e
	6 h			-2.93 ± 0.16^e	72.47 ± 0.15^c	65.69 ± 0.03^a	78.38 ± 0.44^{cde}
	12 h			$-3.74 \pm 0.13d^d$	72.71 ± 0.10^c	63.39 ± 0.15^e	79.53 ± 0.50^{bc}
	18 h			-4.10 ± 0.15^{cde}	72.85 ± 0.00^{bc}	65.86 ± 0.21^{cd}	79.12 ± 0.41^{bcd}
	24 h			-4.48 ± 0.22^{abc}	71.41 ± 0.04^f	62.40 ± 0.31^e	78.02 ± 0.31^{de}
	30 h			-4.68 ± 0.05^{ab}	73.22 ± 0.07^b	64.56 ± 0.16^{bc}	79.83 ± 0.17^b
	36 h			-3.90 ± 0.11^{cd}	72.38 ± 0.00^{cd}	64.89 ± 0.17^{ab}	78.85 ± 0.19^{bcd}
	42 h			-4.88 ± 0.23^a	74.44 ± 0.06^a	65.56 ± 0.18^a	82.31 ± 0.15^a
	48 h			-4.82 ± 0.14^{ab}	71.81 ± 0.00^{ef}	63.37 ± 0.17^d	78.66 ± 0.29^{bcd}
	60 h			-4.78 ± 0.22^{ab}	71.55 ± 0.02^{ef}	65.57 ± 0.14^a	79.18 ± 0.50^{bcd}
	72 h			$-3.98 \pm 0.08de$	72.03 ± 0.00^{ef}	65.56 ± 0.19^{ab}	78.21 ± 0.12^{cde}

Different letters in the same column indicate significant differences ($p < 0.05$). T_0, starting temperature; T_p, peak temperature; T_c, end temperature; ΔH, enthalpy change.

paste. The ΔH is proportional to the degree of relative crystallinity (Luo et al., 2022). As the germination time increased, the termination temperature (T_c) rose from 75.37 ± 0.19 °C at 0 h to 77.99 ± 0.14 °C at 72 h (Table 2). The T_c was greater during germination compared to the starch treatment. In addition, the ΔH of starch enhanced from 6.01 ± 0.10 J/g at 0 h to 9.90 ± 0.16 J/g at 36 h. At 72 h, the ΔH of starch decreased to 7.15 ± 0.29 J/g, exhibiting an initial upward and then a downward trend. This pattern was consistent with the XRD results reported previously. In addition, germination remarkably affected the peak temperature (T_p) of maize starch, which reached a maximum at 48 h. This result may be because of an increase in amylase activity that destroys a few small and weak starch crystals, elevating starch stability and crystal surface energy (Gao et al., 2022). However, after a specific period of germination, post-initial hydrolysis of the amorphous regions, the crystalline regions underwent hydrolysis, subsequently leading to the exposure of the crystalline structure to the endogenous enzymes, reducing the ΔH. Similar results were found in pea starch (Gao et al., 2022).

The onset temperature (T_o), T_p, T_c, and ΔH of ungerminated maize flour were 65.56 ± 0.25 °C, 71.95 ± 0.41 °C, 77.34 ± 0.55 °C, and 2.68 ± 0.61 J/g, respectively (Table 2). The ΔH, T_p, and T_c values initially increased but then decreased with the germination duration. Similar findings were reported in post-germination barley flour, where the T_p and ΔH increased (Al-Ansi et al., 2021). This observation may be attributed to the production of reducing sugars, amino acids, and small molecule polypeptides during maize kernel germination, elevating the T_p of the maize meal. The ΔH is primarily influenced by alterations in the starch structure and protein contents and is generally correlated with the crystallinity and short-ordered structure. In the early stage of maize germination, the starch order briefly improved. However, the enthalpy later decreased, most likely due to prolonged germination. The H-bonds in the double-helix structure were degraded, and the long-branched chains were reduced. Moreover, amylase hydrolyzed the crystalline region of starch, reducing the crystallinity and protein contents.

3.6. Pasting viscosity

The properties of the starch extracted from the ungerminated and germinated maize kernels are listed in Table 3A. The pasting

temperature of maize starch post-germination was conspicuously ($P < 0.05$) higher than that of the starch in the ungerminated maize. Similar results were observed in oats and brown rice (Li, Oh, Lee, Baik, & Chung, 2017). Since hydrolytic enzymes prefer the amorphous regions of starch, this may be related to the formation of a more rigid crystal conformation during maize germination. This activity would enhance the resistance of starch crystals to the infiltration of water molecules and prevent their thermal expansion. The peak viscosity decreased from 3998.0 ± 83.44 to 2807.0 ± 185.26 cP and the final viscosity from 3559.5 ± 53.03 to 1571.0 ± 398.81 cP. Both viscosities diminished remarkably ($P < 0.05$) with germination, which was mainly related to the action of related enzymes and alterations in the molecular weight and chain length of starch granules. The increase in starch disintegration value suggested a decrease in grain viscosity, which may be related to a reduction in the granule size. The regeneration value represents the aging, the degree of aging, and the gelling strength of starch during cooling. Compared to the control group, the viscosity of regeneration diminished from 1432.5 ± 6.36 to 704.0 ± 100.41 cP at 72 h. This decrease in regenerative value indicated the breakdown and degradation of the starch molecular chains, which resulted in a lesser rearrangement during shearing and reduced molecular connectivity. Moreover, this pattern demonstrated that germination inhibits the aging of starch. Earlier studies reported the same trend in brown rice (Zhou et al., 2020).

During the analysis of rapid viscosity monitoring, the viscosity value indicates the resistance of the suspension to the stirring paddle under controlled temperature. The pasting parameters of the maize whole-meal at different germination times are presented in Table 3B. It was evident that the duration of germination markedly reduced the viscosity of the maize whole-meal during pasting ($P < 0.05$). The peak viscosity, setback value, breakdown value, and termination viscosity of maize flour declined from 1904.0 ± 11.0, 3056.5 ± 45.5, 652.0 ± 8.0 and 4308.5 ± 64.5 cP to 70.7 ± 12.9, 46.3 ± 3.7, 15.3 ± 5.2, and 39.7 ± 14.4 cP with prolonging germination after 72 h. A similar trend was also observed in germinated adlay seeds (Xu et al., 2017). The setback, which indicates the degree of aging, is the difference between the termination and initial viscosities. After germination, the setback value reduced remarkably, suggesting an effective inhibition of the regrowth phenomenon in maize flour-based food products. Our findings revealed that the decrease in the viscosity profile of germinated-maize flour was more pronounced compared to maize starch. This observation can be

Table 3
Pasting performance parameters of maize starch with different germination times.

Sample	Germination time	Peak viscosity (cP)	Breakdown (cP)	Setback (cP)	Final viscosity (cP)
Starch	0 h	3998.0 ± 83.44[a]	1471.0 ± 36.77[e]	1432.5 ± 6.36[a]	3559.5 ± 53.03[ab]
	6 h	3669.0 ± 62.23[b]	1452.5 ± 45.96[e]	1463.5 ± 48.8[ab]	3680.0 ± 32.53[a]
	12 h	3670.5 ± 57.5[b]	1568.0 ± 31.11[de]	1500.5 ± 3.53[a]	3603.0 ± 53.74[a]
	18 h	3734.5 ± 85.5[ab]	1747.0 ± 2.83[c]	1470.5 ± 55.86[ab]	3458.0 ± 62.23[ab]
	24 h	3538.0 ± 97.8[b]	1711.0 ± 79.20[cd]	1343.5 ± 14.85[b]	3170.5 ± 0.71[b]
	30 h	3649.5 ± 102.5[b]	1770.5 ± 89.80[bc]	1412.0 ± 1.41[ab]	3291.0 ± 56.57[ab]
	36 h	3074.0 ± 56.6[c]	1912.0 ± 49.50[ab]	1050.5 ± 4.95[c]	2212.5 ± 12.02[c]
	42 h	2829.0 ± 154.15[c]	1776.5 ± 118.09[bc]	715.0 ± 84.85[d]	1767.5 ± 120.92[de]
	48 h	2866.0 ± 36.77[c]	1941.0 ± 12.73[a]	1013.0 ± 0.00[c]	1938.0 ± 24.04[cd]
	60 h	2794.5 ± 200.11[c]	2029.5 ± 6.36[a]	700.5 ± 136.47[d]	1465.5 ± 330.22[e]
	72 h	2807.0 ± 185.26[c]	1940.0 ± 113.14[a]	704.0 ± 100.41[d]	1571.0 ± 398.81[de]
Maize flour	0 h	1904.0 ± 11.0[a]	652.0 ± 8.0[a]	3056.5 ± 45.5[a]	4308.5 ± 64.5[a]
	6 h	1775.5 ± 44.5[a]	591.5 ± 30.5[abc]	1678.5 ± 29.5[bc]	2862.5 ± 43.5[b]
	12 h	1478.7 ± 67.7[b]	443.0 ± 123.5[ab]	2114.3 ± 102.7[b]	3150.0 ± 49.2[b]
	18 h	1129.3 ± 93.9[c]	573.3 ± 263.0[ab]	1508.0 ± 311.0[c]	2241.3 ± 290.5[c]
	24 h	1016.0 ± 64.0[c]	632.5 ± 185.5[abc]	1568.0 ± 324.0[c]	2251.5 ± 502.5[c]
	30 h	663.5 ± 9.5[d]	426.5 ± 7.5[abc]	628.0 ± 5.0[d]	865.0 ± 7.0[d]
	36 h	331.0 ± 9.9[e]	211.0 ± 8.5[bc]	268.7 ± 28.9[de]	388.7 ± 28.0[de]
	42 h	105.5 ± 1.5[f]	62.5 ± 4.5[c]	26.5 ± 4.5[e]	69.5 ± 7.5[e]
	48 h	91.5 ± 5.5[f]	50.0 ± 1.0[c]	25.0 ± 6.0[e]	66.5 ± 10.5[e]
	60 h	93.7 ± 4.3[f]	54.3 ± 4.1[c]	23.0 ± 3.8[e]	62.3 ± 6.4[e]
	72 h	70.7 ± 12.9[f]	46.3 ± 3.7[c]	15.3 ± 5.2[e]	39.7 ± 14.4[e]

Different letters in the same column indicate significant differences ($p < 0.05$).

attributed to the enhanced activities of amylase and protease during grain germination, resulting in reduced starch content, fragmented structure, and increased susceptibility to disintegration during starch emulsion heating. Additionally, the protein structure changed during germination, preventing the formation of a stable protein-starch network structure in the whole maize flour system, reducing the rigidity of the maize paste, and making the system vulnerable to shear action.

3.7. Rheological properties

In dynamic rheology, the energy storage modulus (G′) is often used to describe the elastic behavior of starch gels. G′ is the quantity of the deformation energy that is recovered during each deformation cycle. In contrast, the loss modulus (G″) expresses the viscous behavior of starch gels and represents the amount of energy lost due to viscous dissipative deformation throughout the cycle (Zhang et al., 2022). The ratio of these two moduli is known as the loss angle tangent (tanδ); a tanδ <1 indicates the superiority of the elastic properties of the starch gel over its viscous properties. The tanδ values for all starch samples were < 1, suggesting that the elastic properties of the starch gel were predominant (Fig. 3C).

During maize germination, the G′ of starch initially increased and then decreased, indicating an improvement in the elasticity during the pre-germination period. This change may be associated with alterations in starch crystallinity (Fig. 2A). However, as the degree of germination deepened, G′ and G″ diminished, indicating that germination affects the viscoelastic properties of starch gels. This phenomenon may be attributed to the disruption and rearrangement of long-chain starch molecules in maize caused by germination. Consequently, the relative content of long-chain starch in the system decreases, thereby impacting its viscoelasticity (Jan, Saxena, & Singh, 2018). On the other hand, G″ declined, suggesting that the starch thinned and its mobility was enhanced, which aligns with the previous RVA findings.

The shear stress of starch was directly proportional to the shear rate (Fig. 3D). In contrast, the apparent viscosity of the starch paste was inversely proportional to the germination time, which aligns with the previous findings on the RVA pasting characteristics. The K, n, and R^2 values of the shear stress curve fit are presented in Table S1, with all R^2 values exceeding 0.95, indicating a robust fit. The fitting results reveal a significant reduction in the K values for both the upward and downward lines of the starch thixotropic range. This reduction may be attributed to the degradation of long-chain starch over time, resulting in a structurally weak gel network and reduced resistance to flow. On the other hand, the n value exhibited a decreasing-then-increasing trend after germination. All n values were < 1, indicating a pseudoplastic fluid characteristic. The pseudo-plasticity of the starch paste enhanced within a specific treatment time. Notably, starch solutions with higher n values tend to produce a more viscous feel in the mouth. Therefore, it is advisable to select a viscosity system with a low n value for desirable characteristics.

3.8. In vitro starch digestibility (IVSD)

Fig. 3E depicts the variations in the concentrations of RDS, SDS, and RS at various germination times. As evident from the results, germination remarkably influenced the digestibility of starch. Post-germination, the RDS and SDS levels elevated from 24.16 ± 0.96% to 29.37 ± 0.32% and 28.97 ± 2.30% to 35.27 ± 0.83%, respectively. In contrast, the RS levels dropped dramatically from 46.87 ± 0.96% to 35.37 ± 0.48%, effectively enhancing the digestibility of maize starch.

Starch digestibility depends primarily on the ease of contact between the hydrolase and the starch molecules, whereas changes in the ordered structure play no significant role (Wang, Shi, et al., 2020; Wang, Xiao, et al., 2020; Wang, Xu, et al., 2020). Pits and holes on the starch surface may allow the enzymes to penetrate the granules, thereby increasing digestibility. Germination induces alterations in the metabolism and starch structure, rendering it more susceptible to endogenous enzymes. Starch digestibility can be improved by germination in a variety of cereals, including brown rice, minor millets, and sorghum (Sharma & Gujral, 2020; Marchini et al., 2021; Gui et al., 2021). A decline in the molecular weight and a change in the chain length of starch after germination increased its sensitivity to endogenous enzymes and was a major cause of the elevation in digestibility (Marchini et al., 2021). During seed germination, carbohydrates such as starch are hydrolyzed to D-fructose by starch phosphorylase and invertase and converted by proteolytic enzymes, which are further involved in the production of sucrose via the amino- and nucleotide-sugar, fructose-mannose, galactose, and starch-sucrose metabolic pathways. However, since the production of sucrose does not keep up with its consumption in the galactose and starch-sucrose metabolic pathways, more reserve starch is converted to rapidly digestible starch, which is more readily hydrolyzed, thereby increasing the energy supply to the seed during germination and growth (Dong et al., 2024). Moreover, the surface microstructure of the post-germination maize starch was porous, which enhanced the hydrolytic enzymes–starch contact area and the number of such sites, further elevating the starch–enzyme reaction and enhancing digestibility (Ran, Yang, Chen, & Yang, 2022). Consequently, as germination prolonged,
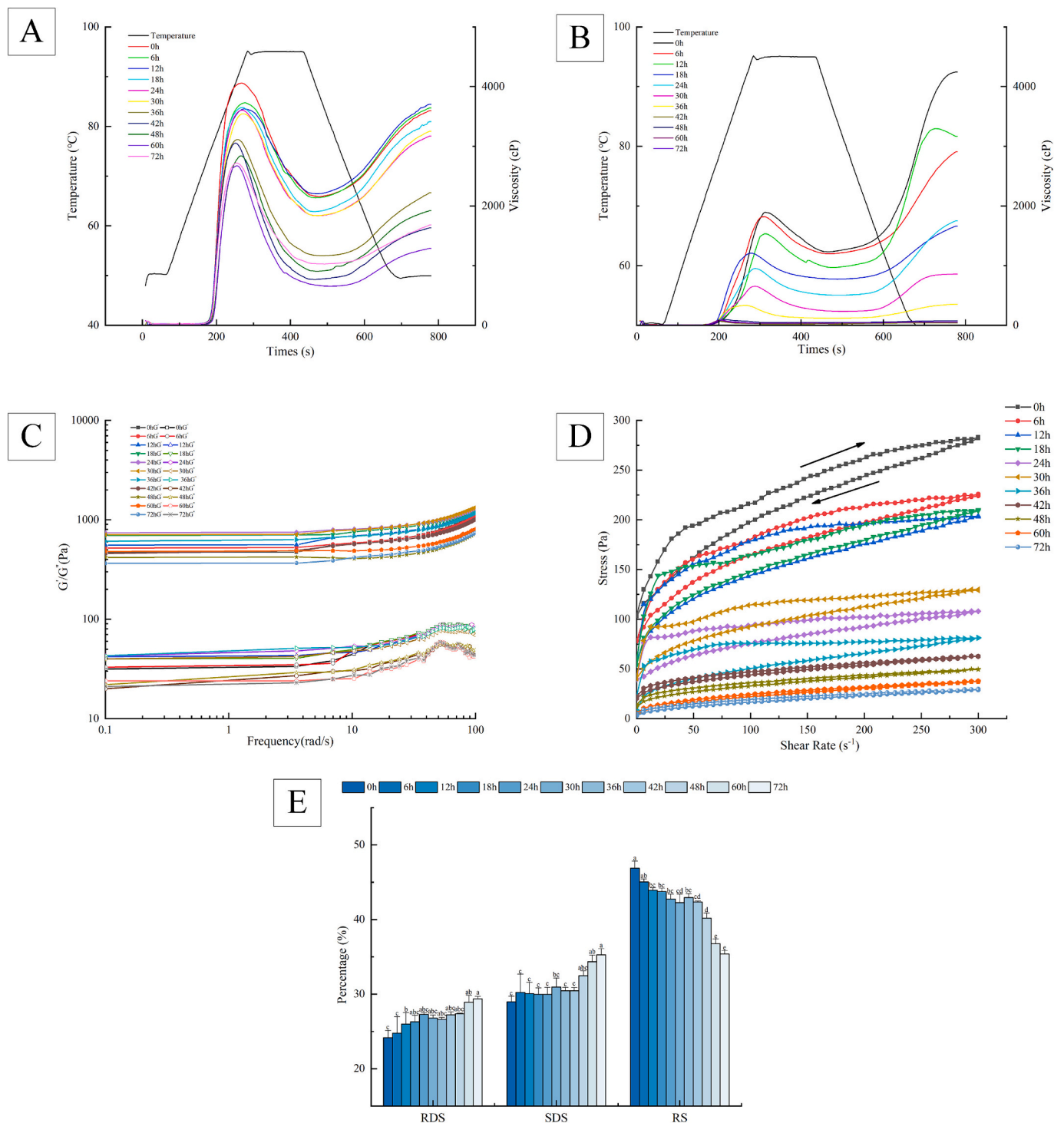
Fig. 3. RVA (A) curves of the maize starch during 0–72 h of germination; RVA (B) curves of the maize flour during 0–72 h of germination; Dynamic rheological characterization of maize starch during 0–72 h of germination (C); Static rheological characterization of maize starch during 0–72 h of germination (D); *In vitro* digestive properties of maize starch during 0–72 h of germination.

the number and size of pores on the starch surface increased, allowing easier access of the enzyme molecules to the binding sites within the starch molecules, resulting in an accelerated rate of enzyme-based structural digestion and a remarkable elevation in the overall digestibility ($P < 0.05$).

3.9. Hydration and gelling properties

The WAI is a measure of the water absorption ability of starch. A higher WAI value indicates a more robust ability of starch to absorb water and form a paste. This ability is primarily influenced by the number of hydrophilic groups present in the maize flour (Singh, Singh, Singh, & Sharma, 2023). The WSI of post-germination maize flour significantly increased ($P < 0.05$) (Table S1). However, the WAI and SP declined compared to the ungerminated maize flour. This pattern can be attributed to the previously insoluble components within the kernel dissolving into soluble small-molecule nutrients upon exposure to enzymes and water during germination. Consequently, the water solubility

index increased from 0.14 ± 0.00 g/g in the ungerminated seeds to 0.49 ± 0.04 g/g post-germination, indicating a greater exposure of small-molecule nutrients, such as amino acids and peptides. The exposure is beneficial for digestion and absorption in the human body, thereby enhancing the digestive properties of germinated maize products to a certain extent (Lemmens et al., 2019). Additionally, the WSI was positively correlated with the viscosity of maize flour, which aligned with the findings from the RVA experiments. A high WAI can result in stickiness during food processing, while a low WAI can lead to turbidity during the cooking process. Therefore, the appropriate processing time should be selected during food production.

The SP of the maize meal diminished from 6.96 ± 0.26 to 4.40 ± 0.36 g/g after 72 h, which was primarily attributed to the structural changes in the starch and proteins, resulting in the formation of a network structure that hindered water absorption and particle swelling. However, the changes in the SP of maize flour during the pre-emergence stage were statistically insignificant, suggesting that appropriate emergence timing during commercial production can enhance the processing performance and nutrient absorption of maize flour.

4. Conclusions

This study examined the impact of germination on the structure, pasting quality, and digestibility of maize starch in relation to the essential nutrients and whole-meal processing characteristics of maize. After 72 h of germination at 25 °C and 75% humidity, the composition and structure of the maize starch changed significantly. Subsequently, as germination progressed, the starch and fat contents of maize kernels declined. In contrast, the protein content reached its maximum value at 36 h. Similarly, the moisture and reducing sugar levels, as well as the activities of two key enzymes, markedly increased. During maize kernel germination, the original protein–starch network structure disintegrated due to the action of various enzymes, and the electrostatic protein–starch interactions weakened, which promoted the hydrophobic interactions and suppressed the formation of the previous dense gluten–starch network structure, which impeded H-bonding between starch and water molecules, and finally lowered the viscosity of the maize starch. Reduced viscosity enhanced the flow properties of the maize starch (Lu, Lee, & Yang, 2022). In addition, the surface of the post-germination maize starch contained more indentations with a higher degree of crystallinity than the starch from ungerminated seeds. However, the crystal structure of the starch remained unchanged. Meanwhile, the short-range ordering decreased with prolonged germination. A similar trend was observed in the peak viscosity of starch and flour; the ΔH also changed. Moreover, germination altered the ratios of the constituents and the digestibility of starch. Germination enhanced the content of water-soluble matter, the WSI, and the digestibility of the maize meal. Thus, post-germinated maize starch can be used to produce food items with low viscosity, such as gluten-free cakes, cookies, *etc.* Therefore, the findings of this study formed a theoretical foundation for germination-based food technology, enabling the structural changes in grain starch and promoting its applicability in the food industry.

CRediT authorship contribution statement

Xin Jiang: Formal analysis, Data curation, Conceptualization. **Yelinxin Chen:** Resources, Formal analysis, Data curation. **Sanabil Yaqoob:** Validation, Supervision, Software. **Lin Xiu:** Writing – review & editing, Writing – original draft, Methodology, Investigation. **Huimin Liu:** Writing – review & editing, Investigation. **Mingzhu Zheng:** Supervision, Project administration, Methodology, Funding acquisition. **Dan Cai:** Supervision, Funding acquisition, Data curation, Conceptualization. **Jingsheng Liu:** Project administration, Methodology, Funding acquisition.

Declaration of competing interest

The authors declare that they have no known competing financial interests or personal relationships that could have appeared to influence the work reported in this paper.

Data availability

Data will be made available on request.

Appendix A. Supplementary data

Supplementary data to this article can be found online at https://doi.org/10.1016/j.fochx.2024.101430.

References

Al-Ansi, W., Mahdi, A. A., Al-Maqtari, Q. A., Sajid, B. M., Al-Adeeb, A., Ahmed, A., … Wang, L. (2021). Characterization of molecular, physicochemical, and morphological properties of starch isolated from germinated highland barley. *Food Bioscience, 42.* https://doi.org/10.1016/j.fbio.2021.101052

AOAC. (2006). *Official Methods of Analysis* (18th Edition). Gaithersburgs, MD: Association of Official Analytical Chemists.

Bai, J. Y., Huang, J. Y., Feng, J. X., Jiang, P. L., Zhu, R., Dong, L. W., Liu, Z. D., Li, L., & Luo, Z. (2023). Combined ultrasound and germination treatment on the fine structure of highland barley starch. *Ultrasonics Sonochemistry, 95,* Article 106394. https://doi.org/10.1016/j.ultsonch.2023.106394

Bravo-Núñez, Á., & Gómez, M. (2019). Physicochemical properties of native and extruded maize flours in the presence of animal proteins. *Journal of Food Engineering, 243,* 49–56. https://doi.org/10.1016/j.jfoodeng.2018.09.005

Chen, L., Tian, Y. Q., Sun, B. X., Cai, C. X., Ma, R. R., & Jin, Z. Y. (2018). Measurement and characterization of external oil in the fried waxy maize starch granules using ATR-FTIR and XRD. *Food Chemistry, 242,* 131–138. https://doi.org/10.1016/j.foodchem.2017.09.016

Dong, Y. Y., Li, Y. L., Su, W. D., Sun, P. D., Yang, H. J., Li, Q., … Yu, X. Z. (2024). Differential metabolic networks in three energy substances of flaxseed (*Linum usitatissimum L.*) during germination. *Food Chemistry, 443,* Article 138463. https://doi.org/10.1016/j.foodchem.2024.138463

Englyst, H. N., Kingman, S. M., & Cummings, J. H. (1992). Classification and measurement of nutritionally important starch fractions. *European Journal of Clinical Nutrition, 46,* S33–S50. https://doi.org/10.1128/IAI.01649-06

Gan, R. Y., Lui, W. Y., Wu, K., Chan, C. L., Dai, S. H., Sui, Z. Q., & Corke, H. (2017). Bioactive compounds and bioactivities of germinated edible seeds and sprouts: An updated review. *Trends in Food Science and Technology, 59,* 1–14. https://doi.org/10.1016/j.tifs.2016.11.010

Gao, L. C., Wu, Y. X., Wan, C. X., Wang, P. K., Yang, P., Gao, X. L., … Gao, J. F. (2022). Structural and physicochemical properties of pea starch affected by germination treatment. *Food Hydrocolloids, 124,* Article 107303. https://doi.org/10.1016/j.foodhyd.2021.107303

Gu, Z. X., Chen, B. C., & Tian, Y. Q. (2021). Highly branched corn starch: Preparation, encapsulation, and release of ascorbic acid. *Food Chemistry, 343,* Article 128485. https://doi.org/10.1016/j.foodchem.2020.128485

Gu, Z. X., Jin, Z., Schwarz, P., Rao, J. J., & Chen, B. J. (2023). Unraveling the role of germination days on the aroma variations of roasted barley malts via gas chromatography-mass spectrometry based untargeted and targeted flavoromics. *Food Chemistry, 426,* Article 136563. https://doi.org/10.1016/j.foodchem.2023.136563

Gui, Y., Zou, F., Li, J., Tang, J., Guo, L., & Cui, B. (2021). Corn starch modification during endogenous malt amylases: The impact of synergistic hydrolysis time of α-amylase and β-amylase and limit dextrinase. *International Journal of Biological Macromolecules,* (190), 819–826. https://doi.org/10.1016/j.ijbiomac.2021.09.052

Hao, Z., Hu, A., Cheng, J., Ma, Z., Li, Z., Lv, J., Xu, H., Ge, H., Wang, H., Yu, Z., Xie, Z., & Du, Y. (2024). Mechanism of interaction between L-theanine and maize starch in ultrasonic field based on DFT calculations: Rheological properties, multi-scale structure and in vitro digestibility. *International Journal of Biological Macromolecules.* https://doi.org/10.1016/j.ijbiomac.2024.129869

Jan, R., Saxena, D. C., & Singh, S. (2018). Comparative study of raw and germinated Chenopodium (Chenopodium album) flour on the basis of thermal, rheological, minerals, fatty acid profile and phytocomponents [J]. *Food Chemistry, 269,* 173–180. https://doi.org/10.1016/j.foodchem.2018.07.003

Lemmens, E., Moroni, A. V., Pagand, J., Heirbaut, P., Ritala, A., Karlen, Y., … Delcour, J. A. (2019). Impact of cereal seed sprouting on its nutritional and

technological properties: A critical review. *Comprehensive Reviews in Food Science and Food Safety, 18*(1), 305–328. https://doi.org/10.1111/1541-4337.12414

Li, C., Oh, S. G., Lee, D. H., Baik, H. W., & Chung, H. J. (2017). Effect of germination on the structures and physicochemical properties of starches from brown rice, oat, sorghum, and millet. *International Journal of Biological Macromolecules*, (105), 931–939. https://doi.org/10.1016/j.ijbiomac.2017.07.123

Liu, X. L., Zhang, J., Yang, X. J., Sun, J. W., Zhang, Y. Y., Su, D. M., … Wang, H. W. (2022). Combined molecular and supramolecular structural insights into pasting behaviors of starches isolated from native and germinated waxy brown rice. *Carbohydrate Ploymers, 283*, Article 119148. https://doi.org/10.1016/j.carbpol.2022.119148

Liu, Y., Su, C. Y., Saleh, A. S. M., Wu, H., Zhao, K., Zhang, G. Q., Jiang, H., Yan, W. J., & Li, W. H. (2020). Effect of germination duration on structural and physicochemical properties of mung bean starch. *International Journal of Biological Macromolecules, 154*, 706–713. https://doi.org/10.1016/j.ijbiomac.2020.03.146

Lu, Z., Lee, P. R., & Yang, H. S. (2022). Chickpea flour and soy protein isolate interacted with κ-carrageenan via electrostatic interactions to form egg omelets analogue. *Food Hydrocolloids, 130*, Article 107691. https://doi.org/10.1016/j.foodhyd.2022.107691

Luo, X. Y., Li, D. D., Tao, Y., Wang, P., Yang, R. Q., & Han, Y. B. (2022). Effect of static magnetic field treatment on the germination of brown rice: Changes in α-amylase activity and structural and functional properties in starch. *Food Chemistry, 383*, Article 132392. https://doi.org/10.1016/j.foodchem.2022.132392

Ma, X. H., Liu, Y., Liu, J. S., Zhang, J. J., & Liu, R. N. (2020). Changes in starch structures and in vitro digestion characteristics during maize (Zea mays L.) germination. *Food Science & Nutrition, 8*, 1700–1708. https://doi.org/10.1002/fsn3.1457

Ma, Y. X., Chen, Z. D., Wang, Z. P., Chen, R. X., & Zhang, S. G. (2023). Molecular interactions between apigenin and starch with different amylose/amylopectin ratio revealed by X-ray diffraction, FT-IR, and solid-state NMR. *Carbohydrate Polymers., 310*, Article 120737. https://doi.org/10.1016/j.carbpol.2023.120737

Marchini, M., Marti, A., Folli, C., Prandi, B., Ganino, T., Conte, P., … Carini, E. (2021). Sprouting of Sorghum (*Sorghum bicolor* [L.] Moench): Effect of drying treatment on protein and starch features. *Foods, 10*, 407. https://doi.org/10.3390/foods10020407

Najib, T., Heydari, M. M., Tu, K., & Meda, V. (2023). Modification in starch structure of soaked and germinated lentil seeds under various thermal processing methods, including conventional, microwave, and microwave-assisted techniques. *Food Chemistry Advances, 2*, Article 100267. https://doi.org/10.1016/j.focha.2023.100267

Nieves-Hernández, M. G., Correa-Piña, B. L., Esquivel-Fajardo, E. A., Barrón-García, O. Y., Gaytán-Martínez, M., & Rodriguez-Garcia, M. E. (2023). Study of morphological, structural, pasting, thermal, and vibrational changes in maize and isolated maize starch during germination. *Journal of Cereal Science, 111*, Article 103685. https://doi.org/10.1016/j.jcs.2023.103685

Oliveira, M. E. A. S., Coimbra, P. S. S., Galdeano, M. S., Carvalho, C. W. P., & Takeiti, C. Y. (2020). How does germinated rice impact starch structure, products and nutrional evidences? – A review. *Trends in Food Science and Technology, 12*, 13–23. https://doi.org/10.1016/j.tifs.2022.02.015

Prasanna, B. M., Palacios-Rojas, N., Hossain, F., Muthusamy, V., Menkir, A., Dhliwayo, T., … Fan, X. (2020). Molecular breeding for nutritionally enriched maize: Status and prospects. *Frontiers in Genetics, 10*, 1392. https://doi.org/10.3389/fgene.2019.01392

Ran, X. L., & Yang, H. S. (2022). Promoted strain-hardening and crystallinity of a soy protein-konjac glucomannan complex gel by konjac glucomannan. *Food Hydrocolloids, 133*, Article 107959. https://doi.org/10.1016/j.foodhyd.2022.107959

Ran, X. L., Yang, Z. X., Chen, Y. F., & Yang, H. S. (2022). Konjac glucomannan decreases metabolite release of a plant-based fishball analogue during in vitro digestion by affecting amino acid and carbohydrate metabolic pathways. *Food Hydrocolloids, 129*, Article 107623. https://doi.org/10.1016/j.foodhyd.2022.107623

Sharma, B., & Gujral, S. H. (2020). Modifying the dough mixing behavior, protein & starch digestibility and antinutritional profifile of minor millets by sprouting. *International Journal of Biological Macromolecules, 153*, 962–970. https://doi.org/10.1016/j.ijbiomac.2019.10.225

Singh, G., Singh, B., Singh, A., & Sharma, S. (2023). Functionality of barley pasta supplemented with Mungbean flour: Cooking behavior, quality characteristics and morphological interactions. *Journal of Food Measurement and Characterization, 17*, 5806–5820. https://doi.org/10.1007/s11694-023-02080-

Su, C., Saleh, A. S. M., Zhang, B., Feng, D., Zhao, J., Guo, Y., … Yan, W. (2020). Effects of germination followed by hot air and infrared drying on properties of naked barley flour and starch. *International Journal of Biological Macromolecules, 165*(15), 2060–2070. https://doi.org/10.1016/j.ijbiomac.2020.10.114

Wang, H., Xu, K., Liu, X., Zhang, Y., Xie, X., & Zhang, H. (2020). Understanding the structural, pasting and digestion properties of starch isolated from frozen wheat dough. *Food Hydrocolloids, 111*, Article 106168. https://doi.org/10.1016/j.foodhyd.2020.106168

Wang, H. W., Xiao, N. Y., Ding, J. T., Zhang, Y. Y., Liu, X. L., & Zhang, H. (2020). Effect of germination temperature on hierarchical structures of starch from brown rice and their relation to pasting properties. *International Journal of Biological Macromolecules, 147*, 965–972. https://doi.org/10.1016/j.ijbiomac.2019.10.063

Wang, R. M., Chen, P., He, T. S., Zhan, B., & Bai, B. (2022). The influence mechanism of brown rice starch structure on its functionality and digestibility under the combination of germination and zinc fortification. *Foodservice Research International, 161*, Article 111825. https://doi.org/10.1016/j.foodres.2022.111825

Wang, X. F., Shi, Y. N., Chen, Y., Fan, J. P., Pu, Y. H., & Huang, A. X. (2020). Comparative proteome analysis of matured dry and germinating *Moringa oleifera* seeds provides insights into protease activity during germination. *Foodservice Research International, 136*, Article 109332. https://doi.org/10.1016/j.foodres.2020.109332

Xing, X., Teng, C., Sun, M. H., Zhang, Q. P., Zhou, B. W., Cui, H. L., … Qin, P. Y. (2021). Effect of germination treatment on the structural and physicochemical properties of quinoa starch. *Food Hydrocolloids, 115*, Article 106604. https://doi.org/10.1016/j.foodhyd.2021.106604

Xu, L., Chen, L., Ali, B., Yang, N., Chen, Y. S., Wu, F. F., … Xu, X. M. (2017). Impact of germination on nutritional and physicochemical properties of adlay seed (*Coixlachryma-jobi L.*). *Food Chemistry, 229*, 312–318. https://doi.org/10.1016/j.foodchem.2017.02.096

Xu, M. W., Jin, Z., Gu, Z. X., Rao, J. J., & Chen, B. C. (2020). Changes in odor characteristics of pulse protein isolates from germinated chickpea, lentil, and yellow pea: Role of lipoxygenase and free radicals. *Food Chemistry, 314*, Article 126184. https://doi.org/10.1016/j.foodchem.2020.126184

Xu, M. W., Jin, Z., Simsek, S., Hall, C., Rao, J. J., & Chen, B. C. (2019). Effect of germination on the chemical composition, thermal, pasting, and moisture sorption properties of flours from chickpea, lentil, and yellow pea. *Food Chemistry, 295*, 579–587. https://doi.org/10.1016/j.foodchem.2019.05.167

Zhang, K., Zhang, Z., Zhao, M., Milosavljević, V., Cullen, P. J., Scally, L., … Tiwari, B. K. (2022). Low-pressure plasma modification of the rheological properties of tapioca starch [J]. *Food Hydrocolloids, 125*. https://doi.org/10.1016/j.foodhyd.2021.107380

Zhang, Y., Xing, B. F., Kong, D. G., Gu, Z. X., Yu, Y. J., Zhang, Y. J., & Li, D. D. (2024). Improvement of in vitro digestibility and thermostability of debranched waxy maize starch by sequential ethanol fractionation. *International Journal of Biological Macromolecules, 254*, Article 127895. https://doi.org/10.1016/j.ijbiomac.2023.127895

Zhou, L., Lu, Y., Zhang, Y., Zhang, C., Zhao, L., Yao, S., Sun, X., Chen, T., Zhu, Z., Zhao, Q., Zhao, C., Liang, W., Lu, K., Wang, C., & Liu, Q. (2020). Characteristics of grain quality and starch fine structure of *japonica* rice kernels following preharvest sprouting. *Journal of Cereal Science, 95*, Article 103023. https://doi.org/10.1016/j.jcs.2020.103023